

# Correlated defects, metal-insulator transition, and magnetic order in ferromagnetic semiconductors

C. Timm,\* F. Schäfer, and F. von Oppen

*Institut für Theoretische Physik, Freie Universität Berlin, Arnimallee 14, D-14195 Berlin, Germany*

(Dated: January 22, 2002)

The effect of disorder on transport and magnetization in ferromagnetic III–V semiconductors, in particular (Ga,Mn)As, is studied theoretically. We show that Coulomb-induced correlations of the defect positions are crucial for the transport and magnetic properties of these highly compensated materials. We employ Monte Carlo simulations to obtain the correlated defect distributions. Exact diagonalization gives reasonable results for the spectrum of valence-band holes and the metal-insulator transition only for correlated disorder. Finally, we show that the mean-field magnetization also depends crucially on defect correlations.

PACS numbers: 75.50.Pp, 71.30.+h, 72.20.Ee

*Introduction.*—Recently, there has been substantial interest in diluted ferromagnetic III–V semiconductors due to observations of relatively high Curie temperatures [1, 2, 3]. This makes these materials promising for applications as well as interesting from the physics point of view. They could allow the incorporation of ferromagnetic elements into semiconductor devices, and thus the integration of processing and magnetic storage on a single chip. To be specific, we consider here manganese-doped GaAs. The properties of this material rely on the dual role played by the Mn impurities: They carry a local spin due to their half-filled d-shell and dope the system with holes, which mediate a ferromagnetic indirect exchange interaction between the spins. Furthermore, the materials are highly compensated presumably due to antisite defects (As substituted for Ga) [4, 5], which drives them towards a metal-insulator transition (MIT). It is clearly important to understand the interplay between transport properties, magnetic ordering, and the defect configuration. In this letter we show that *correlated* defects are required for a description consistent with experiments.

There is a growing body of theoretical work on (Ga,Mn)As, for a review see Ref. [6]. Most approaches fall into two categories in that they start either from the heavily doped regime [7, 8, 9, 10, 11, 12, 13], where one considers a high density of holes in the valence band, or from the weak-doping limit [14, 15], where the impurity states form an impurity-band. In the case of heavy doping [7, 8, 9, 10, 11, 12, 13] one considers valence-band holes moving in the disorder potential of the defects. For large hole concentration the Fermi energy  $E_F$  lies deep in the valence band compared to the Coulomb-potential fluctuations and the latter are neglected. It is not clear whether this is justified for (Ga,Mn)As. On the other hand, for light doping [14, 15] the local impurity states overlap only weakly, forming an impurity band. We have pointed out [16] that this model is problematic since for the typical doping range the impurity band would be much broader than the energy gap. Both approaches have in common that antisite defects and correlations of

defects are neglected.

The outline of the remainder of this paper is as follows. First, we discuss the configuration of Mn impurities and antisite defects with the help of Monte Carlo simulations and obtain the disorder potential and its spatial correlations. Then, we derive the spectrum and localization properties of holes in this potential and discuss the MIT. Finally, we calculate the polarizations of Mn and hole spins within a selfconsistent mean-field theory and discuss our results.

*Defect configurations.*—In the theory of doped semiconductors one often assumes the dopants to be randomly distributed [6, 17]. However, for high compensation only few charge carriers are present, which only weakly screen the Coulomb interaction between charged defects [17]. Experiments [5] suggest that defects diffuse rapidly at 250°C, which is a typical growth and annealing temperature for (Ga,Mn)As grown by molecular beam epitaxy. This diffusion leads to screening of the Coulomb potential *by the ions*. Following Keldysh and Proshko [18] we assume that the defects come into thermal equilibrium during growth and that the resulting configuration is quenched at low temperatures.

To find typical defect configurations close to equilibrium we perform Monte Carlo simulations for Mn impurities and antisites. Relative to Ga, Mn impurities have charge  $-e$  while antisites carry  $+2e$ . The weak screening by the holes is included by means of a screening length  $r_{\text{scr}}$  obtained from nonlinear screening theory [17].  $r_{\text{scr}}$  is much larger than the nearest-neighbor separation of Ga sites for realistic parameters so that it hardly affects the small-scale defect correlations, which mostly determine the physics. We show below that  $r_{\text{scr}}$  is also much larger than the screening length  $r_{\text{ion}}$  due to defect diffusion. We employ the Metropolis algorithm at 250°C for systems of  $20 \times 20 \times 20$  conventional cubic unit cells with periodic boundary conditions, unless stated otherwise.

A typical result for Mn concentration  $x = 0.05$  and  $p = 0.3$  holes per Mn is shown in Fig. 1: Most of the defects have formed clusters. We emphasize that this is

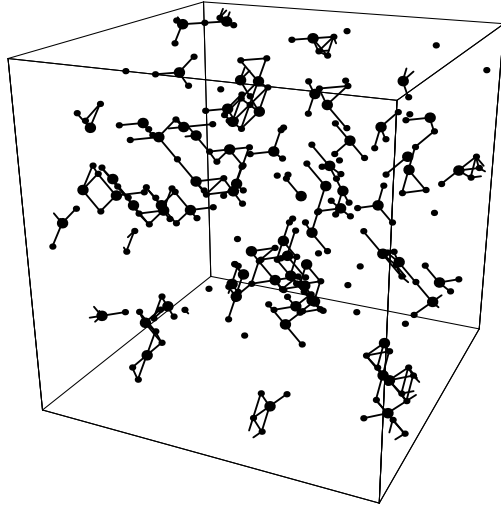


FIG. 1: Typical equilibrium configuration at 250°C for 5% Mn doping and 0.3 holes per Mn. Only the defects are shown, large (small) circles denote antisite (Mn) defects. Defects at nearest neighbor Ga sites are connected by a bond. For clarity of presentation, we show only  $10 \times 10 \times 10$  conventional unit cells.

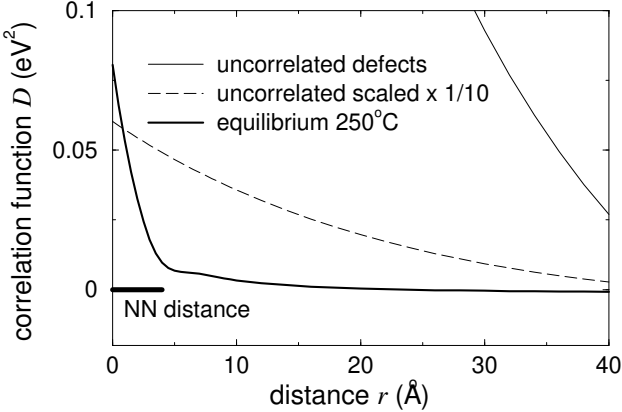


FIG. 2: Potential correlation function  $D(r)$  for 5% Mn and 0.3 holes per Mn, both for uncorrelated defects and for equilibrium at the growth temperature. The nearest-neighbor Ga site separation of 3.99 Å is also indicated.

only possible due to the presence of antisites. The cluster formation leads to the screening of the disorder potential, as can be seen from the potential correlation function  $D(r) \equiv \langle V(\mathbf{r}) V(\mathbf{r}') \rangle_{|\mathbf{r}-\mathbf{r}'|=r} - \langle V \rangle^2$  plotted in Fig. 2 for  $x = 0.05$  and  $p = 0.3$ . Note that  $\sqrt{D(0)} \equiv \Delta V$  is the width of the distribution of  $V(\mathbf{r})$ . For correlated defects,  $D(r)$  and thus  $\Delta V$  are strongly reduced and correlations of  $V(\mathbf{r})$  decay on the much shorter length scale  $r_{\text{ion}}$ , which is of the order of the nearest-neighbor Ga site separation [19]. Importantly, however,  $\Delta V \approx 0.284$  eV is still *not* small compared to the Fermi energy  $|E_F| \approx 0.329$  eV.

It is interesting to note that correlated defects are a

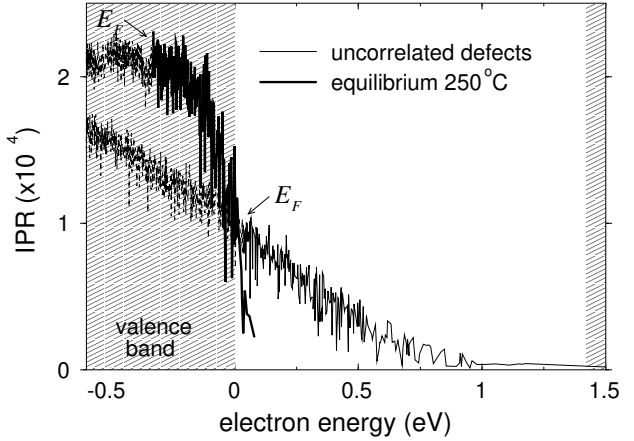


FIG. 3: IPR as a function of energy for the valence-band edge for 5% Mn and 0.3 holes per Mn. The thin (heavy) solid line denotes occupied states for uncorrelated (correlated) defects, the dotted lines denote empty states.

special feature of ferromagnetic III-V semiconductors. Mn dopants in II-VI materials do not carry charge.

*Hole states.*—The next step is to find the spectrum and localization properties of the valence-band holes moving in the disorder potential  $V(\mathbf{r})$ . We start from the Hamiltonian  $H = -\sum_i (\hbar^2/2m^*) \nabla_i^2 + V(\mathbf{r}_i)$ , where we use the envelope function and parabolic-band approximations [20]. The calculations are done for spin-less holes, which is justified since the additional disorder introduced by the exchange interaction with the Mn spins is much smaller than  $\Delta V$ .

The Hamiltonian is solved by exact diagonalization in a plane-wave basis, giving the energy spectrum and normalized eigenfunctions. From these we obtain the inverse participation ratio  $\text{IPR}(n) = 1/\sum_{\mathbf{r}} |\psi_n(\mathbf{r})|^4$  of the states  $\psi_n(\mathbf{r})$ . The IPR allows one to estimate the position of the mobility edge, since it is of the order of the volume for extended states but falls below it for localized states.

Figure 3 shows a comparison of the IPR as a function of energy for uncorrelated defects and for the equilibrium configuration obtained above, both for 5% Mn and 0.3 holes per Mn. We plot electron energies increasing to the right. It is obvious that, firstly, the valence-band edge is strongly smeared out by uncorrelated defects so that the energy gap is completely filled, whereas correlated defects only lead to a small tail in the gap. Secondly, the states close to the band edge are much more localized for uncorrelated defects, due to the larger disorder potential. The Fermi energy  $E_F$  would in this case lie among states showing a tendency towards localization. On the other hand, for correlated defects the states close to  $E_F$  are clearly extended. Thus, both the spectrum and the localization properties agree with experiments only for correlated defects.

In Fig. 4 we show the IPR as a function of energy for correlated defects at various Mn dopings and hole con-

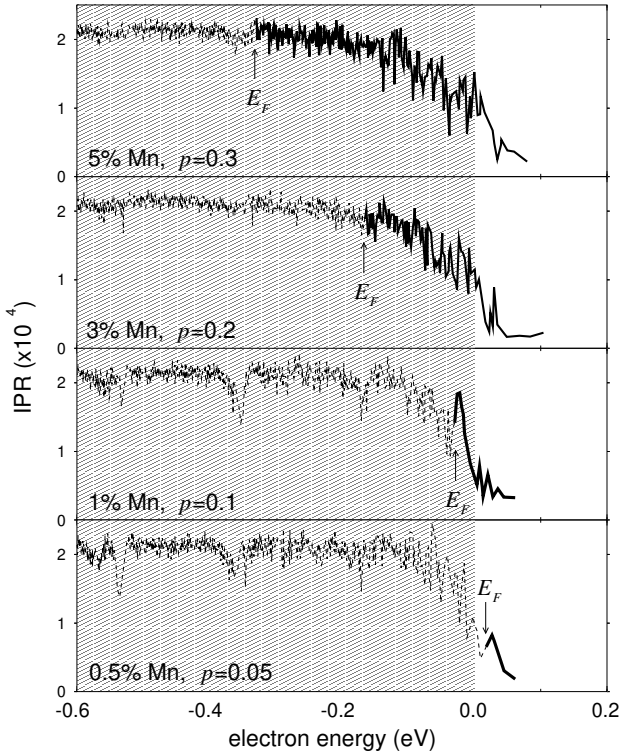


FIG. 4: IPR as a function of electron energy for the valence-band edge for various Mn dopings and hole concentrations  $p$  per Mn taken from experiment [1, 21].

centrations. The dependence of the hole concentration on the Mn doping was chosen to be consistent with experiments [1, 21]. The spectrum and the IPR change little with Mn doping—disorder is only slightly stronger for large doping. The reason for this small effect is that the potential screened by the defects on the length scale  $r_{\text{ion}}$  is much less affected by a change of concentration than the bare Coulomb potential.

The dominant effect comes from the hole concentration. For 3% and 5% Mn, the states at  $E_F$  are extended and we expect metallic behavior. Thus here the neglect of the impurity potential should be a reasonable approximation. For 1% Mn,  $E_F$  lies within states with intermediate IPR, while for 0.5% Mn, it is clearly in the localized tail. From this we expect the MIT to take place at a Mn concentration of the order of 1%. In view of our approximation this result is in reasonable agreement with experiments [1]. For comparison, note that uncorrelated defects would lead to an MIT at about 5% Mn, see Fig. 3.

**Magnetization.**—Finally, we discuss the spontaneous magnetization and its dependence of the defect configuration. The exchange interaction between hole and Mn spins is described by the Hamiltonian  $H = -\sum_i (\hbar^2/2m^*) \nabla_i^2 + V(\mathbf{r}_i) - J_{\text{pd}} \sum_{i,l} \mathbf{s}_i \cdot \mathbf{S}_l \delta(\mathbf{r}_i - \mathbf{R}_l)$ , where  $V(\mathbf{r})$  is the disorder potential obtained above,  $J_{\text{pd}} \approx -45 \text{ eV } \text{\AA}^3$  is the exchange integral [10, 22, 23],  $\mathbf{s}_i$  and  $\mathbf{S}_l$  are the hole and Mn spin operators, respec-

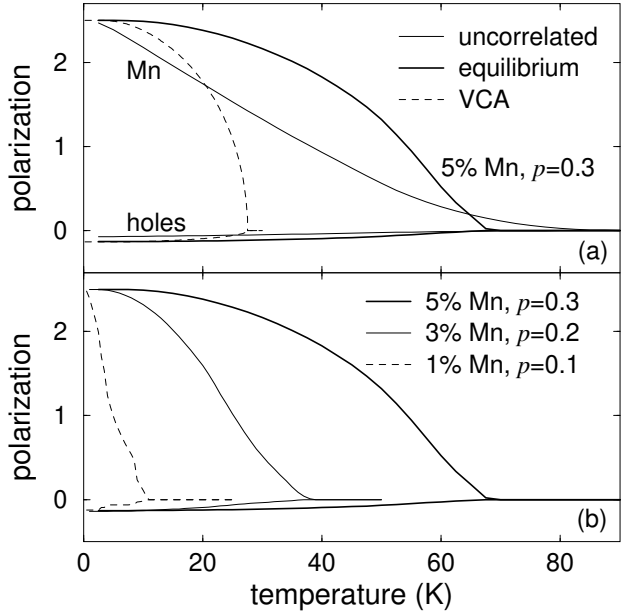


FIG. 5: (a) Magnetization as a function of temperature for 5% Mn and 0.3 holes per Mn, both for uncorrelated and correlated defects. The results denoted by “VCA” neglect disorder. (b) Magnetization for various Mn and hole concentrations (with correlated defects).

tively, and  $\mathbf{R}_l$  are the Mn impurity positions. In second quantized form, the Hamiltonian reads

$$H = \sum_{n\sigma} c_{n\sigma}^\dagger \epsilon_n c_{n\sigma} - J_{\text{pd}} \sum_{n\sigma, n'\sigma'} \sum_l c_{n\sigma}^\dagger \psi_n^*(\mathbf{R}_l) \frac{\boldsymbol{\tau}_{\sigma\sigma'}}{2} \cdot \mathbf{S}_l \psi_{n'}(\mathbf{R}_l) c_{n'\sigma'},$$

where  $\epsilon_n$  are the eigenenergies obtained in the absence of exchange as discussed above,  $\psi_n(\mathbf{r})$  are the corresponding eigenfunctions, and  $\boldsymbol{\tau}$  is the vector of Pauli matrices. The exchange interaction is decoupled at the mean-field level, introducing the averaged Mn spin polarizations  $\mathbf{M}_l \equiv \langle \mathbf{S}_l \rangle$  and hole spin polarizations at the Mn sites,  $\mathbf{m}_l \equiv \langle \sum_{n\sigma, n'\sigma'} c_{n\sigma}^\dagger \psi_n^*(\mathbf{R}_l) (\boldsymbol{\tau}_{\sigma\sigma'}/2) \psi_{n'}(\mathbf{R}_l) c_{n'\sigma'} \rangle$ . We do *not* perform a spatial average, *i.e.*, the disorder is retained. The hole and Mn sectors can now be diagonalized separately,  $\mathbf{M}_l$  and  $\mathbf{m}_l$  are calculated, and the procedure is iterated. This selfconsistent mean-field theory is similar to the one employed by Berciu and Bhatt [14]. The main difference is that we start from realistic hole states for the disorder potential.

Figure 5(a) shows the Mn and hole spin polarizations for  $x = 0.05$  and  $p = 0.3$ . Also shown are the polarizations obtained neglecting disorder by using plane waves for the hole states and the virtual crystal approximation (VCA) for the Mn spins [6, 8, 20]. We see that disorder strongly enhances  $T_c$ , as proposed in Ref. [14]. This increase of  $T_c$  by a factor of more than two is easily understood in mean-field theory:  $T_c$  is determined

by the indirect exchange interaction of nearest-neighbor Mn pairs. Without disorder, the typical distance is  $r_{\text{vca}} \sim n_{\text{Mn}}^{-1/3}$ , where  $n_{\text{Mn}}$  is the density of Mn impurities. For  $x = 0.05$ ,  $r_{\text{vca}} \sim 9.67 \text{ \AA}$ . On the other hand, with disorder the nearest-neighbor separation on the Ga sublattice is  $r_{\text{dis}} = 3.99 \text{ \AA}$ . If we assume RKKY-type indirect exchange [7, 8, 9], the exchange interaction behaves as  $1/r$  for small separations. Then the indirect exchange, and thus  $T_c$ , is larger by a factor of  $r_{\text{vca}}/r_{\text{dis}} \sim 2.4$  in the disordered case.

For *correlated* defects the polarization curve looks quite “mean-field-like,” in qualitative agreement with experiments [1, 11, 24]. This can be explained by the extended nature of the relevant hole states for correlated defects, which leads to a long-range indirect exchange interaction. Thus the effective field seen by a Mn spin  $\mathbf{S}_i$  is averaged over many other Mn spins and the spatial fluctuations of this effective field are small. On the other hand, for *uncorrelated* defects the holes are partly localized, the indirect exchange is of shorter range, and the fluctuations of the effective field are larger. We believe that this leads to the smeared-out magnetization curve for uncorrelated defects. Also, the mean-field  $T_c$  is slightly higher in this case because the indirect exchange interaction between nearest-neighbor spins is larger for uncorrelated defects, since there are hole states localized in the vicinity of the pair. It is clearly important to study the effect of fluctuations on the magnetization. We expect fluctuations to reduce  $T_c$  in particular for the uncorrelated case. We will address this question elsewhere.

Figure 5(b) shows that  $T_c$  is reduced for smaller Mn and hole concentrations. This trend follows the disorder-free theory [6, 8]. Note also that in all cases the holes are only partially polarized. For 1% Mn we observe instabilities due to nearly degenerate saddle points, which are also typical for the impurity-band approach.  $T_c$  is approximately proportional to the Mn concentration  $x$ , in accordance with experiments [1].

To conclude, we have obtained typical defect configurations in (Ga,Mn)As and studied the effect of the resulting disorder potential on the valence-band holes. We argue that the defect positions are highly correlated due to screening of their large Coulomb interactions by defect diffusion at the growth temperature. The previously neglected antisite defects are crucial for this mechanism. We have shown that such a correlated distribution of defects is required to understand the hole spectrum, the metal-insulator transition, and the shape of the magnetization curves. Our results should also help to clarify why the properties of ferromagnetic semiconductors depend so strongly on details of the growth process.—We profited from discussions with A. Chudnovskiy, P. J. Jensen, J. König, J. Schliemann, and in particular M. E. Raikh,

who emphasized the importance of compensation.

---

\* Electronic address: timm@physik.fu-berlin.de

- [1] H. Ohno, Science **281**, 951 (1998); H. Ohno, J. Magn. Magn. Mat. **200**, 110 (1999); H. Ohno and F. Matsukura, Solid State Commun. **117**, 179 (2001).
- [2] H. Ohno *et al.*, Appl. Phys. Lett. **69**, 363 (1996); F. Matsukura *et al.*, Phys. Rev. B **57**, R2037 (1998).
- [3] M. L. Reed *et al.*, Appl. Phys. Lett. **79**, 3473 (2001).
- [4] M. Luysberg *et al.*, Mater. Res. Soc. Symp. Proc. **442**, 485 (1997).
- [5] S. J. Potashnik *et al.*, Appl. Phys. Lett. **79**, 1495 (2001); see also R. C. Lutz *et al.*, Physica B **273–274**, 722 (1999).
- [6] J. König *et al.*, cond-mat/0111314.
- [7] T. Dietl, A. Haury, and Y. Merle d’Aubigné, Phys. Rev. B **55**, R3347 (1997); T. Dietl *et al.*, Science **287**, 1019 (2000).
- [8] T. Jungwirth *et al.*, Phys. Rev. B **59**, 9818 (1999).
- [9] J. König, H.-H. Lin, and A. H. MacDonald, Phys. Rev. Lett. **84**, 5628 (2000); in *Interacting Electrons in Nanostructures*, edited by R. Haug and H. Schoeller, Lecture Notes in Physics **579** (Springer, Berlin, 2001), p. 195, cond-mat/0010471; J. König, T. Jungwirth, and A. H. MacDonald, Phys. Rev. B **64**, 184423 (2001).
- [10] M. Abolfath *et al.*, Phys. Rev. B **63**, 054418 (2001).
- [11] T. Dietl, H. Ohno, and F. Matsukura, Phys. Rev. B **63**, 195205 (2001).
- [12] A. Chattopadhyay, S. Das Sarma, and A. J. Millis, Phys. Rev. Lett. **87**, 227202 (2001).
- [13] J. Schliemann and A. H. MacDonald, cond-mat/0107573.
- [14] M. Berciu and R. N. Bhatt, Phys. Rev. Lett. **87**, 107203 (2001); cond-mat/0111045.
- [15] A. L. Chudnovskiy and D. Pfannkuche, cond-mat/0108396.
- [16] C. Timm, F. Schäfer, and F. von Oppen, submitted to Phys. Rev. Lett. (comment), cond-mat/0111504; M. Berciu and R. N. Bhatt, submitted to Phys. Rev. Lett. (reply), cond-mat/0112165.
- [17] B. I. Shklovskii and A. L. Efros, *Electronic Properties of Doped Semiconductors*, Solid-State Sciences **45** (Springer, Berlin, 1984).
- [18] L. V. Keldysh and G. P. Proshko, Sov. Phys.—Solid State **6**, 1093 (1964–1965).
- [19] The electronic screening length  $r_{\text{scr}}$  decreases for reduced disorder potential. However,  $r_{\text{ion}}$  is always the smaller, and thus relevant, length scale.
- [20] For quantitative material-specific calculations the light and split-off bands could be incorporated using the Kohn-Luttinger Hamiltonian [10, 11]. This should not change the qualitative results but is known to increase the mean-field  $T_c$  [11]. We leave this extension as work for the future.
- [21] F. Matsukura *et al.*, Phys. Rev. B **57**, R2037 (1998).
- [22] J. Okabayashi *et al.*, Phys. Rev. B **58**, R4211 (1998).
- [23] A. K. Bhattacharjee and C. Benoit à la Guillaume, Solid State Commun. **113**, 17 (2000).
- [24] B. Beschoten *et al.*, Phys. Rev. Lett. **83**, 3073 (1999).